Review Article

Imperatives of Mathematical Model of Arterial Blood Dynamics for Interpretation of Doppler Velocimetry: A Narrative Review

Umar Abubakar[1]*, Anthony Chukwuka Ugwu[2], Godwin Christopher Ezike Mbah[3], Tertsegha Tivde[4], Mohammed Sidi[5], Geofery Luntsi[6], Kalu Ochie[7], Alhaji Modu Ali[8], Anas Mohammed[9]

[1]Department of Radiography, College of Health Sciences, Usmanu Danfodiyo University, Sokoto, Nigeria, [2]Department of Radiography and Radiation Sciences, Nnamdi Azikiwe University, Awka, Nigeria, [3]Department of Mathematics, University of Nigeria, Nsukka, Nigeria, [4]Department of Mathematics, University Agriculture, Makurdi, Nigeria, [5]Department of Medical Radiography, College of Medical Sciences, Bayero University, Kano, Nigeria, [6]Department of Medical Radiography, College of Medical Sciences, University of Maiduguri, Maiduguri, Nigeria, [7]Department of Radiography and Radiation Sciences, Evangel University Akaeze, Akaeze, Ebonyi State, Nigeria, [8]Department of Radiology, Federal Neuro-Psychiatric Hospital, Maiduguri, Nigeria, [9]Department of Radiology, Specialist Hospital Gombe, Maiduguri, Nigeria

Abstract

Clinicians frequently study arterial Doppler velocimetric waveforms depicted by Doppler sonography of the kidneys, the heart, the brain, and the feto-maternal circulation to assess the well-being of the aforementioned vital organs. The waveform interpretation of the Doppler indices can be studied using a mathematical model. The developed models serve as teaching tools and for easy comprehension of the regulatory mechanism of the organs. It will also obtain accurate wall shear stress (WSS) and likely atherosclerotic sites can be predicted early. The aim of this review is to reveal the imperatives of mathematical models in the study of the physical interpretation of Doppler velocimetry. The models will explore sonographic Doppler velocimetry and computational fluid dynamics (CFD) in determining the segments of the arteries that are prone to the development of atheromatous plaque. It will be achieved by comparing and computing the measurement differences of the WSS. A thorough literature review was carried out between 1971 and 2021 on the mathematical modeling of blood dynamics and Doppler velocimetry of different blood vessels, across various electronic databases including NC AHEC Digital Library, PUBMED, ERIC, MEDLINE, Free Medical Journals, and EMBASE. The results of the literature search were presented using the PRISMA flow chat. The narrative review of the mathematical models of arterial blood dynamics is based on incompressible Navier-Stokes equations, the Windkessel model, and CFD. It was deduced that the blood flow velocity decreased with time across the varying frequency from 0.2Hz to 0.50Hz in the interlobar arterial channels. The review also revealed that adult humans' Doppler indices of the renal-interlobar artery agree with developed models of renal interlobar arterial blood dynamics. The mathematical model measurements of the great vessels matched the sonographic Doppler velocimetry with <15% variation. In our fast-paced world of epidemiological transition, the imperatives of mathematical modeling of arterial flow dynamics based on the Navier–Stokes equations to represent various physiologic and pathologic situations cannot be overstated. The practical consequences include the possibility of mathematical models to acquire precise WSS distribution and early detection of potential atherosclerotic sites during cardiovascular Doppler sonography.

Keywords: Blood dynamic, Doppler velocimetry, mathematical model

Introduction

Doppler velocimetry delineates characteristics and direction of blood dynamics**,** which is utilized in the evaluation of arterial supply to the kidney, brain, heart, feto-maternal circulations, etc.[1-3] Sonographic Doppler velocimetry is a diagnostic tool that gives the clinicians a clue about the well-being of the aforementioned organs.[4,5] Vascular resistance can be estimated by hemodynamic (the science that describes the physics of blood flow) indices based on Maximal systolic velocity, minimal diastolic velocity, end-diastolic velocity, and mean velocity.[6] The Doppler indices are calculated from the arteries of the kidney, brain, heart feto-maternal circulations to reveal the hypoxic states of Newtonian blood flow. Doppler

Received: 05-02-2023 **Revised:** 28-02-2023 **Accepted:** 17-03-2023 **Available Online:** 23-06-2023

Access this article online

Quick Response Code:

Website: https://journals.lww.com/jmut

DOI: 10.4103/jmu.jmu_8_23

Address for correspondence: Dr. Umar Abubakar, Department of Radiography, College of Health Sciences, Usmanu Danfodiyo University, Sokoto, Nigeria. E-mail: umar.abubakar5@udusok.edu.ng

How to cite this article: Abubakar U, Ugwu AC, Mbah GC, Tivde T, Sidi M, Luntsi G, *et al*. Imperatives of mathematical model of arterial blood dynamics for interpretation of Doppler velocimetry: A narrative review. J Med Ultrasound 2023;31:188-94.

velocimetry of the renal and umbilical arterial blood dynamic provides an indirect measure of renal and placental functions.[7] Increase in systolic-to-diastolic ratio and decreased diastolic flow suggest increased renal vascular resistance and renal compromise. When the umbilical Doppler indices are severely abnormal (increased or decreased pulsatility and resistive indices) is an indicator of poor antenatal prognosis.[8-11] It is also noteworthy that when the Doppler indices become abnormal, it usually accompanies congenital abnormalities, which are taken into consideration during antenatal management.[12,13] In a systematic review,[14-16] evidence revealed that it is imperative to carry out Doppler sonography of the feto-maternal arterial circulation of pregnancies with high risk and poor prognosis.[17-19] However, much needs to be learned about the rheology of the cardiovascular system and the etiology of its pathologic conditions. The investigation and early prediction of the disease conditions of the cardiovascular system are carried out by a powerful tool known as a mathematical model.[17,20,21] The mathematical model can be defined as a system or powerful tool that utilizes mathematical language and concepts.[22] A mathematical model or modeling is the process involved in developing a model which can be used to validate a concept. It helps in explaining the effects of Newtonian behavior of plasma and erythrocytes on the blood vessels by measuring wall shear stress (WSS) distribution and to make early predictions on the atheromatous plaque, constrictions, aneurysms, or atresia.[22-27] Doppler sonography displays the real-time measurement of blood dynamic velocimetry and spectral analysis of cardiovascular circulation. This generates detailed data on the blood flow velocimetry against the arterial walls.[28-33] There are challenges in correlating the obtained data to physiological variables of the cardiovascular system. First, the clinicians find it challenging to connect the rigorous mathematical model that describes the pulsatility and resistivity of arterial blood dynamic and the pathological conditions.[17,28] Second, the separation of the Doppler data acquisition and processing methodology from that of physical meaning. The mathematical modeling can eliminate methodological factors. Doppler ultrasound is a diagnostic imaging modality that extensively reveals cardiovascular disease, and for the evaluation of renal, brain, heart, uteroplacental, and fetal circulations.[4,8-10,17] The main merit of the mathematical model is that the pressure and instantaneous pulsatile and resistive flow of blood in the arteries can be calculated.[17,22,24] The calculated data from the model of the arterial blood dynamics can be used for the interpretation of Doppler velocimetry of human kidneys, brain, heart, and fetus in determining their physiological and pathological conditions. It helps to analyze the blood flow dynamics through a constricted and dilated blood vessel. This is achieved by studying the WSS distribution of the blood vessels and the impedance in the constricted or dilated regions.

The mathematical modeling of arterial blood dynamics using computational fluid dynamics (CFD) allows a wider range analysis of arterial flow phenomena.[28] Doppler velocimetry in combination with CFD and WSS distribution are useful diagnostic tools for determining renal, coronary, and carotid arterial segments prone to atheromatous plaque development.[34-38] WSS is the force per unit area the blood flow exerts on the tunica intima of the blood vessels. It plays an important role in the pathophysiology of atheromatous plaque formation and atherosclerosis. The endothelial cells sensed the changes in WSS due to variations in the flow of erythrocytes and plasma. This will trigger the release of vasodilators and vasoconstrictors.[28,39] The endothelial WSS of relatively straight arteries are unidirectional and pulsatile, while the WSS of arteries with irregular geometry is oscillatory.[28] Magnetic resonance velocimetry (MRV) using phase contrast magnetic resonance imaging (PC-MRI) and sonographic Doppler velocimetry have been used to study arterial WSS.[37-44] This review aims at using a mathematical model of arterial blood dynamics to study Doppler velocimetry. Using CFD and MATLAB, the velocimetry of the blood dynamics and WSS will be measured using an incompressible NSE.[29,45,46] The measurements obtained from the Doppler velocimetry will be compared with the obtained values from the modeled arterial blood flow and CFD.

Methods

A thorough literature review was carried out between 1971 and 2021 on the mathematical modeling of blood dynamics and Doppler velocimetry of different blood vessels, across various electronic databases including NC AHEC Digital Library, PUBMED, ERIC, MEDLINE, Free Medical Journals, and EMBASE.[47] Many pieces of literature that revealed the imperatives of the mathematical models of arterial blood dynamics for the interpretation of Doppler velocimetry were explored. These include mathematical models of feto-maternal circulation, renal interlobar artery, carotid artery, fetal heart, and umbilico–placental circulation among others. The search results of the review are presented in a PRISMA flow chart [Figure 1 and Table 1].

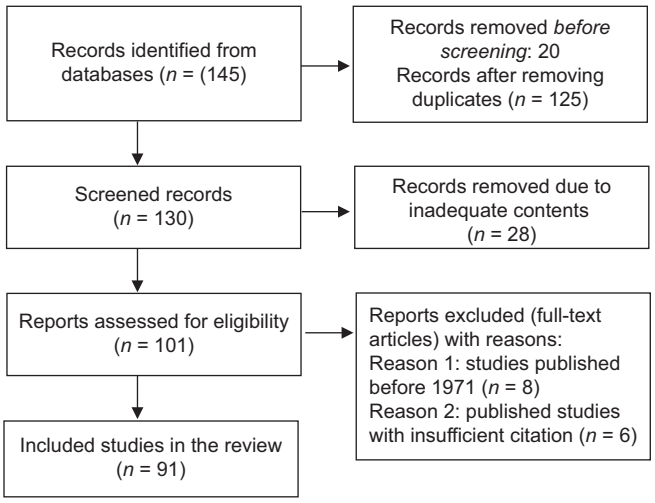

Figure 1: The articles' flowcharts, which were used in the narrative review

Table 1: Literature reviewed and the emerging themes

Authors	Major emerging themes
Thompson *et al*.,[4,8-11] Giles.,[7] Trudinger *et al*.,[11]	Mathematical model for interpretation of doppler velocimetry
Onwuzu *et al*.,[28] Gates *et al*.,[37] Irace *et al*.,[38] Sui *et al*.,[44] Poelma *et al*.,[62,63] Fraser *et al*.,[64] Von *et al*.,[65]	Mathematical model (WSS and CFD) versus ultrasound Doppler
Ali *et al*.,[22], Sahu *et al*.,[23] Kumar and Kumar[24] Sankar *et al*.,[25] Nardinochini *et al*.,[26] Takuji *et al*.,[27]	Modeling of Newtonian and nonNewtonian tapered arterial blood dynamics
Me´nigault *et al*.,[17] Guettouche *et al*.,[18] Guiot *et al*.,[19] Guiot C *et al*.,[20] Hill *et al*.,[21]	Doppler measurements compared to the mathematical model

WSS: wall shear stress, CFD: Computational fluid dynamics

Mathematical model of arterial and bifurcation segments of the feto-maternal circulation[17-19]

It consists of arterial and bifurcation segments. The equations of the model are governed by Navier–Stokes fluid mechanics and formulated based on the law of conservation of mass. In addition, Newtonian behavior of plasma and erythrocytes in the blood vessels was considered. The arterial elasticity was incorporated and blood was considered incompressible while arterial blood pressure and dynamic were assumed to be constant. Based on these assumptions, the law of conservation of mass equation can be written as follows:

$$\frac{\partial(\upsilon S)}{\partial z}+\frac{\partial S}{\partial t}+\Psi=0 \quad (1)$$

$$\frac{\partial \upsilon}{\partial t}+\upsilon\frac{\partial \upsilon}{\partial x}+\frac{1\partial p}{\rho\partial z}=-f \quad (2)$$

$$c_2=\frac{s}{\rho\frac{\partial s}{\partial p}} \quad (3)$$

$$c(p,z)=c_1(p)\times c_2(z) \quad (4)$$

$$c_1(p)=(a_1+a_2p+a_3p^2) \quad (5)$$

Where

υ = mean blood flow velocity

S = cross-section of the artery

z = distance from the arterial tree to the aortic valve

ψ = the function of the small arterial outflow (geometrically non-depicted)

ρ = density (mass per unit volume m/v) of the blood

p = exerted pressure (force per unit area F/A) on the artery

f = WSS

c = pressure wave velocity c (for arterial vascular elasticity)[17-19]

Fetal heart modeling

The equation below demonstrates the relationship between ventricular volume and pressure:[17,20-21]

$$p(t)=E(t)\left[V(t)-Vo\right] \quad (6)$$

$$E(t)=E_{\max}E_n(t) \quad (7)$$

$$En(tn)=5.412t_n^6-20.066t_n^5+25.542t_n^4-13.714t_n^3-1.085t_n+0.029 \quad (8)$$

$$P_{ps}=E_{\max}\left[V_{ps}-V_o\right] \quad (9)$$

Where

$p(t)$ = ventricular pressure (mmHg)

$V(t)$ = volume of blood in the ventricle (mL)

Vo = volume reference value

$E(t)$ = elastance of the ventricle

$E_n(t)$ = elastance in normalized state (amplitude)

E_{max} = arterial contractility at maximum (mmHg ml^{-1})

$E_n(t/T_{\max})$ = elastance in normalized state (amplitude and time)

$T_{\max}$ = maximum time between onset of cardiac and end-systolic velocity

T_n = time in normalized state

P_{ps} and V_{ps} = exerted pressure and volume of blood in the ventricle maximum systole[17,20,21]

Mathematical model of the peripheral area

$$Q(t)=\frac{p(t)-p_c}{R}+C\frac{dp(t)}{dt} \quad (10)$$

Pc, C, and R = critical pressure, compliance, and resistance of the peripheral areas. They were determined by blood flow velocities of fetal Doppler sonography (Doppler indices of the peripheral areas).[17,19,20]

Mathematical model (wall shear stress of carotid artery)[28,31-35]

$$\rho\frac{\partial \upsilon_r}{\partial t}=\frac{\partial p}{\partial r}\mu\left(\frac{\partial^2\upsilon r}{\partial r^2}+\frac{1}{2}\frac{\partial \upsilon_r}{\partial r}-\frac{\upsilon r}{r^2}+\frac{\partial^2\upsilon r}{\partial z^2}\right) \quad (11)$$

$$\rho\frac{\partial \upsilon_r}{\partial t}=-\frac{\partial p}{\partial r}\mu\left(\frac{\partial^2\upsilon r}{\partial r^2}+\frac{1}{2}\frac{\partial \upsilon_z}{\partial r}-\frac{\upsilon r}{r^2}+\frac{\partial^2\upsilon r}{\partial z^2}\right) \quad (12)$$

$$\frac{\partial \upsilon_r}{\partial z}+\frac{\partial \upsilon_z}{\partial z}+\frac{\upsilon_r}{r}=0 \quad (13)$$

The equation for calculating WSS:

$$f=\mu\times\frac{\partial t}{\partial r} \quad (14)$$

f = the WSS

μ = blood viscosity

υ = arterial blood velocity

r = arterial wall radius[28,31-35]

Mathematical model of the renal interlobar artery[48,49]

$$\left.\begin{aligned}\frac{\partial u}{\partial t}&=\frac{\partial p}{\partial r}+\frac{\upsilon_0 R_0}{\mu}\left[\frac{\partial^2 u}{\partial r^2}+\frac{\partial u}{r\partial r}-\frac{u}{r^2}+\frac{\partial_2 u}{\partial z^2}\right]\\ \frac{\partial u}{\partial t}&=-\frac{\partial p}{\partial r}+\frac{\upsilon_0 R_0}{\mu}\left[\frac{\partial^2 \upsilon}{\partial r^2}+\frac{\partial \upsilon}{r\partial r}+\frac{\partial^2 \upsilon}{\partial z^2}\right]\\ \frac{1}{r}\frac{\partial}{\partial r}&\left[ru(t,r,z)\right]+\frac{\partial \upsilon}{\partial z}=0\end{aligned}\right\}^{[50,51]} \quad (15)$$

Model for interpretation of Doppler velocimetry in umbilico–placental circulation

$$PI=\frac{2p_1}{p_0}\left(1+\frac{R_2}{R_1}\right)\left(\frac{1+(\omega R_2 C)^2}{1+(R_2/R_1)^2+(\omega R_2 C)^2}\right)^{1/2} \quad (16)$$

$$PI_p=\frac{2p_1}{p_0}\left(1+\frac{R_2}{R_1}\right)\left(\frac{1}{1+R_2/R_1)^2+(\omega R_2 C)^2}\right)^{1/2} \quad (17)$$

$$PI\rightarrow\frac{2p_1}{p_0}\left(1+\frac{R_2}{R_1}\right) \quad (18)$$

Where PI = pulsatility index[4,8-10]

Results/Discussions

Any location along the umbilico–placental arterial tree can have its instantaneous blood pressure and velocity calculated using the developed mathematical model.[17-19] The arterial tree's pressure levels are generally constant and range between a systolic value of 55 mmHg and a diastolic value of 35 mmHg.[17,20-22] The umbilical artery and the mean pressure of ascending aorta decreased by 10 mmHg at the insertion of the placenta (cord). These findings concur with observations of pregnant women and *in vivo* physiological pressure measurements on lamb and human fetuses. Blood velocities were measured using Doppler velocimetry at key places on human uterine and fetal arteries. The computed findings computed instantaneous flow profiles, and the Doppler velocimetry observations are in good agreement. The Doppler spectral envelope and the estimated blood velocity profiles are analogous.[17,20-22] The kidneys, heart, placenta, etc., are irrigated by blood dynamics in a high continuous component, while the femoral and external iliac arteries are irrigated by blood dynamics that present a low continuous component which displayed two regions with different hemodynamic resistances.[17] The hemodynamic resistance indices are reflected in the shapes of the velocity profiles. The peak systolic velocity and end diastolic velocity of the blood, which are frequently employed by obstetricians to assess fetal well-being, are used to calculate the indices.[52,53] Physiological resistive and pulsatility indices can be found in the computed arterial blood dynamics. The *in vivo* physiological and computational data accord with the computed distribution of flows along the feto-maternal arterial tree. The physiological and bifurcation segments combine to provide the foundation of the proposed model of arterial circulation.[20,21] Any arterial tree can be developed using this mathematical model, which was used to study feto-maternal arterial circulation. The curves of the computed instantaneous pressure and velocity were compared to published data on human and animal fetuses (measured at the umbilical cord at parturition). The velocities and the obtained Doppler velocity data were compared. The calculated physiological outcomes concur with the measurements of arterial blood dynamics measurement taken on gravid women that are healthy.[17,20-22]

The first stage in developing the mathematical model of the renal interlobar artery was the consideration of the flow process in the interlobar artery as shown in Figure 2. The tapering shape of the renal interlobar artery was also considered as shown in Figure 3. In the first 0.2 s, at a variable frequency of 0.20 Hz–0.50 Hz, the blood dynamic velocity in the interlobar artery increased from 400 mm/s to a maximum of 500 mm/s, then fell as the frequency of flow increased across the arterial channel. This trend is seen by increasing the time of flow. The pulsatility of the blood flow in the artery caused the velocity to continue moving in a wavelike pattern. The time-averaged intensity-weighted mean velocity (TAVmean) and the time-averaged maximal velocity (TAVmax) were calculated using the *in vivo* physiological renal interlobar indices (TAVmean). The TAVmax was computed by summing the area above the curve for negative velocities and the area under the curve for positive velocities, then dividing by the R-R interval. The TAV was calculated during diastole and the entire cardiac cycle using the second retrograde flow. Due to the pressure gradient produced by tissue ischemia, capillary dilatation, and decreased peripheral resistance during hyperemia, the flow velocities rose and the waveform altered from triphasic to monophasic with the continuous anterograde flow. Further research revealed that blood flow pressure drops in a wave-like pattern as artery radius increases.[46,47] Only the recoil of blood flow (backflow), which is consistent with

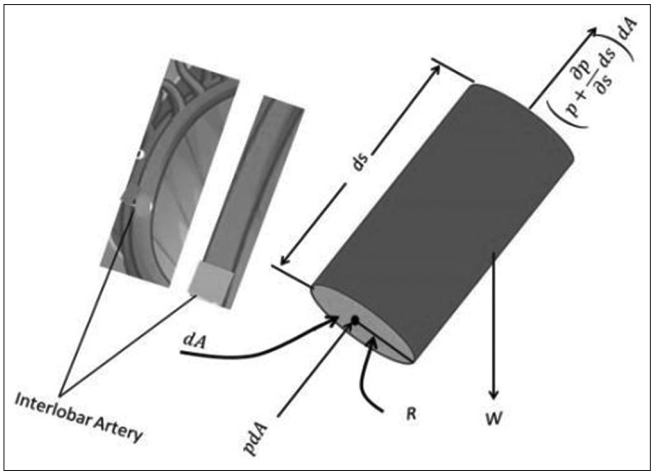

Figure 2: The flow process in the interlobar artery

Olowoyeye *et al*., allowed for the observation of this pattern.[30] Therefore, the heart's pumping motion, the conduit arteries' elastic recoil, and the resistance of the distal microvasculature affect the blood flow within the interlobar artery.[54,55] Thus, Olowoyeye *et al.* findings are supported by the quantification of blood flow as a function of mean blood velocity and the area across the interlobar artery.[30] The obtained Doppler indices of the renal interlobar artery from adult humans agree with the developed model of the renal interlobar artery.[48,49] The resistive index (RI) and pulsatility index (PI) are the Doppler indices for the kidneys.[1,51-53] In adults, an RI value of 0.70 is typically regarded as normal, with a mean value of 0.60 ± 0.01 (mean ± standard deviation).[1,51-53] In chronic renal failure, the normal range for PI value (1.36 and 1.56) would be increased, and it is correlated with the filtration fraction, the resistance of renal vasculature, and effective renal plasma flow.[1,51-53] The physiological interlobar arterial blood velocity profiles are similar to the Doppler spectral envelopes both in normal and abnormal renal Doppler indices [Figure 4].

The researchers obtained measurements from carotid Doppler velocimetry and the developed mathematical model, as well as percentage differences at various arterial segments.[28,37,38] The carotid bulb exhibited the lowest WSS values, whereas the common carotid artery had the highest WSS values. The WSS values for the model were calculated during a period of three consecutive heartbeats. To validate the model, the clinical measurements obtained from human participants are expected to match the results of end-diastolic velocity and peak systolic velocity, with a measurement of a percentage difference of not more than 15%.[28,44,56-59] Clinical measurements consistently produced lower values than the mathematical model. The percentage difference between the external carotid artery and the carotid bulb was greater than 15%. The peak systolic and end-diastolic velocities across the carotid artery were measured clinically and matched the CFD data.[28,50] The peak and average WSS values for the carotid bulb were 1.39 N/cm^2 and 3.13 1.34 N/cm^2, for the common carotid they were 19.81 N/cm^2 and 15.76 1.81 N/cm^2, and for the external carotid, they were 11.51 N/cm^2 and 8.05 1.65 N/cm^2. The Doppler velocimetry observations and the model measurements were within 15% variation. The obtained measurements of Doppler velocimetry were lower compared to the values for the mathematical model based on WSS. The carotid bulb has low WSS distribution, making the segment most susceptible to atheromatous plaque development. The practical consequences include the possibility of using mathematical models to acquire precise WSS distribution and early detection of potential atherosclerotic portions during cardiovascular Doppler sonography.[28,37,38,44,56-59]

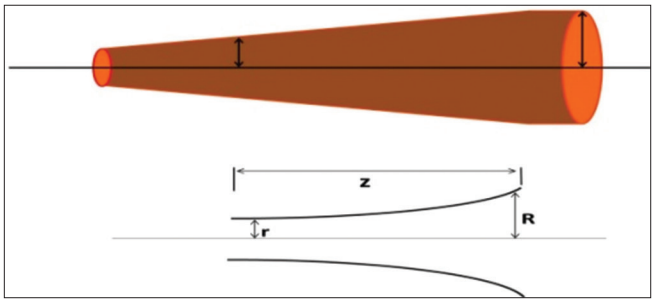

Figure 3: The flow process in the interlobar artery (tapered in shape)

In a study that used a mathematical model to examine the interpretation of empirical Doppler indices (RI and PI), the placenta and its complex branching (placental villous bed) were modeled in great detail.[7,8] The disease condition of the placental vasculature was modeled either as a fractional decrease in the radius of the vessels or as an effaced portion of the terminal branches.[8,10] The developed model can reproduce or simulate the arterial waveforms of both the typical and aberrant umbilical arteries. Theoretical relationships between the bulged arterial resistances and capacitance and the velocity waveform indices were obtained for different input pressure functions. The ratio between the placenta and umbilical artery resistances is approximately proportional to the umbilical Doppler indices. The PI determines the pulsatility of the input pressure waveform. The Fourier PI was examined for an arbitrary pressure function, and the umbilical arterial waveform behaves like (PI).[2] It was concluded that there was a wide range variation of umbilico–placental Doppler indices with the ratio of the arterial umbilical resistance and the arterial placental resistance (R2/R1, including the presence of extensive vascular diseases.[8-11] The models help to predict disease incidence such as atherosclerotic sites, frequency, and severity, especially in the new normal with a fast-paced epidemiological transition.

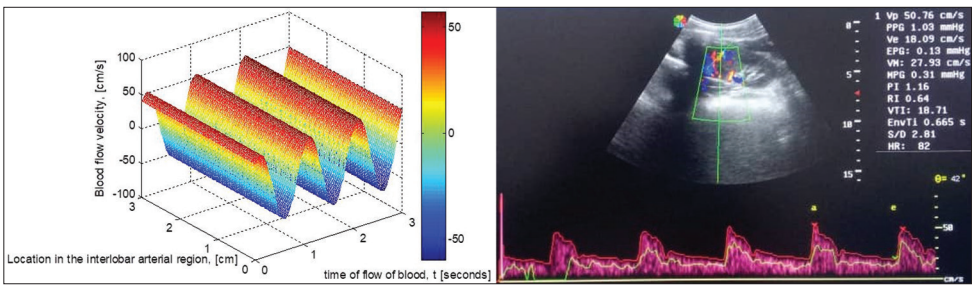

Figure 4: The three-dimensional variation in the flow velocity across the interlobar arterial cross-sectional area and the Doppler indices of the left interlobar artery. The waveform clearly outlines the pulsatility nature of the renal interlobar artery.[1,50,51,57]

Conclusions

In our fast-paced world of epidemiological transition, the imperatives of mathematical modeling of arterial flow dynamics based on the Navier–Stokes equations to represent various physiologic and pathologic situations cannot be overstated. The practical consequences include the possibility of mathematical models to acquire precise WSS distribution and early detection of potential atherosclerotic sites during cardiovascular Doppler sonography.

Financial support and sponsorship

Nil.

Conflicts of interest

There are no conflicts of interest.

References

1. Sidi M, Ugwu AC, England A, Manafa PO, Dambatta AH, Zira JD, *et al.* Renal doppler indices and their correlation with laboratory indices of human immunodeficiency virus sero-positive adult individuals. Radiography (Lond) 2021;27:1014-20.
2. Taori KB, Chaudhary RS, Attarde V, Dhakate S, Sheorain V, Nimbalkar P, *et al.* Renal Doppler indices in sickle cell disease: Early radiologic predictors of renovascular changes. AJR Am J Roentgenol 2008;191:239-42.
3. Viazzi F, Leoncini G, Derchi LE, Pontremoli R. Ultrasound Doppler renal resistive index: A useful tool for the management of the hypertensive patient. J Hypertens 2014;32:149-53.
4. Thompson RS, Stevens RJ. Mathematical model for interpretation of Doppler velocity waveform indices. Med Biol Eng Comput 1989;27:269-76.
5. Gill RW, Trudinger BJ, Garrett WJ, Kossoff G, Warren PS. Fetal umbilical venous flow measured in utero by pulsed Doppler and B-mode ultrasound. I. Normal pregnancies. Am J Obstet Gynecol 1981;139:720-5.
6. McArthur C, Geddes CC, Baxter GM. Early measurement of pulsatility and resistive indexes: Correlation with long-term renal transplant function. Radiology 2011;259:278-85.
7. Giles WB, Trudinger BJ, Baird PJ. Fetal umbilical artery flow velocity waveforms and placental resistance: Pathological correlation. Br J Obstet Gynaecol 1985;92:31-8.
8. Thompson RS, Trudinger BJ, Cook CM. A comparison of Doppler ultrasound waveform indices in the umbilical artery – I. Indices derived from the maximum velocity waveform. Ultrasound Med Biol 1986;12:835-44.
9. Thompson RS, Trudinger BJ, Cook CM. A comparison of Doppler ultrasound waveform indices in the umbilical artery – II. Indices derived from the mean velocity and first moment waveforms. Ultrasound Med Biol 1986;12:845-54.
10. Thompson RS, Trudinger BJ, Cook CM. Doppler ultrasound waveform indices: A/B ratio, pulsatility index and Pourcelot ratio. Br J Obstet Gynaecol 1988;95:581-8.
11. Trudinger BJ, Giles WB, Cook CM, Bombardieri J, Collins L. Fetal umbilical artery flow velocity waveforms and placental resistance: Clinical significance. Br J Obstet Gynaecol 1985;92:23-30.
12. Tublin ME, Bude RO, Platt JF. Review. The resistive index in renal Doppler sonography: Where do we stand? AJR Am J Roentgenol 2003;180:885-92.
13. Radermacher J, Mengel M, Ellis S, Stuht S, Hiss M, Schwarz A, *et al.* The renal arterial resistance index and renal allograft survival. N Engl J Med 2003;349:115-24.
14. Radermacher J, Chavan A, Bleck J, Vitzthum A, Stoess B, Gebel MJ, *et al.* Use of Doppler ultrasonography to predict the outcome of therapy for renal-artery stenosis. N Engl J Med 2001;344:410-7.
15. Crutchley TA, Pearce JD, Craven TE, Stafford JM, Edwards MS, Hansen KJ. Clinical utility of the resistive index in atherosclerotic renovascular disease. J Vasc Surg 2009;49:148-55.
16. Radermacher J, Ellis S, Haller H. Renal resistance index and progression of renal disease. Hypertension 2002;39:699-703.
17. Ménigault E, Berson M, Vieyres P, Lepoivre B, Pourcelot D, Pourcelot L. Feto-maternal circulation: Mathematical model and comparison with Doppler measurements. Eur J Ultrasound 1998;7:129-43.
18. Guettouche A, Challier JC, Ito Y, Papapanayotou C, Cherruault Y, Azancot-Benisty A. Mathematical modeling of the human fetal arterial blood circulation. Int J Biomed Comput 1992;31:127-39.
19. Guiot C, Piantà PG, Todros T. Modelling the feto-placental circulation: 1. A distributed network predicting umbilical haemodynamics throughout pregnancy. Ultrasound Med Biol 1992;18:535-44.
20. Todros T, Guiot C, Piantà PG. Modelling the feto-placental circulation: 2. A continuous approach to explain normal and abnormal flow velocity waveforms in the umbilical arteries. Ultrasound Med Biol 1992;18:545-51.
21. Hill AA, Surat DR, Cobbold RS, Langille BL, Mo LY, Adamson SL. A wave transmission model of the umbilicoplacental circulation based on hemodynamic measurements in sheep. Am J Physiol 1995;269:R1267-78.
22. Ali A, Hussain M, Anwar MS, Inc M. Mathematical modeling and parametric investigation of blood flow through a stenosis artery. Appl Math Mech Engl Ed 2021;42:1675-84.
23. Sahu MK, Sharma SK, Agrawal AK. Study of arterial blood flow in stenosed vessel using non-Newtonian couple stress fluid model. Int J Dyn Fluids 2010;6:209-18.
24. Kumar S, Kumar S. A Mathematical model for Newtonian and non-Newtonian flow through tapered tube. Int Rev Pure Appl Math 2009;15:09-15.
25. Sankar DS, Hemalatha K. A non-Newtonian fluid flow model for blood flow through a catheterized artery-steady flow. Appl Math Model 2007;31:1847-64.
26. Nardinochini P, Pontrelli G, Teresi L. A one-dimensional model for blood flow in pre stressed vessel. Eur J Mech 2005;24:23-33.
27. Takuji I, Guimaraes FR. Effect of non-Newtonian property of blood on flow through a stenosed tube. Fluid Dyn Res 1998;22:251-64.
28. Onwuzu SW, Ugwu AC, Mbah GC, Elo IS. Measuring wall shear stress distribution in the carotid artery in an African population: Computational fluid dynamics versus ultrasound Doppler velocimetry. Radiography (Lond) 2021;27:581-8.
29. McDonald DA. Blood Flow in Arteries. 2nd ed. London: Edward Arnold; 1971.
30. Olowoyeye OA, Gar-Wai Chiu SE, Wright GA, Moody AR. Analysis of the velocity profile of the popliteal artery and its relevance during blood flow studies. J Diagn Med Sonogr 2017;33:489-97.
31. Wentzel JJ, Chatzizisis YS, Gijsen FJ, Giannoglou GD, Feldman CL, Stone PH. Endothelial shear stress in the evolution of coronary atherosclerotic plaque and vascular remodelling: Current understanding and remaining questions. Cardiovasc Res 2012;96:234-43.
32. Krams R, Cuhlmann S, Foin N, Evans P. Shear stress, inflammation and Atherosclerosis. Artery Res 2010;4:41-6.
33. Koskinas KC, Feldman CL, Chatzizisis YS, Coskun AU, Jonas M, Maynard C, *et al.* Natural history of experimental coronary atherosclerosis and vascular remodeling in relation to endothelial shear stress: A serial, *in vivo* intravascular ultrasound study. Circulation 2010;121:2092-101.
34. Stroev PV, Hoskins PR, Easson WJ. Distribution of wall shear rate throughout the arterial tree: A case study. Atherosclerosis 2007;191:276-80.
35. Blake JR, Meagher S, Fraser KH, Easson WJ, Hoskins PR. A method to estimate wall shear rate with a clinical ultrasound scanner. Ultrasound Med Biol 2008;34:760-74.
36. Carvalho JL, Nielsen JF, Nayak KS. Feasibility of *in vivo* measurement of carotid wall shear rate using spiral Fourier velocity encoded MRI. Magn Reson Med 2010;63:1537-47.
37. Gates PE, Gurung A, Mazzaro L, Aizawa K, Elyas S, Strain WD, *et al.* Measurement of wall shear stress exerted by flowing blood in the human carotid artery: Ultrasound Doppler velocimetry and echo particle image velocimetry. Ultrasound Med Biol 2018;44:1392-401.

38. Irace C, Carallo C, De Franceschi MS, Scicchitano F, Milano M, Tripolino C, *et al.* Human common carotid wall shear stress as a function of age and gender: A 12-year follow-up study. Age (Dordr) 2012;34:1553-62.
39. Chatzizisis YS, Coskun AU, Jonas M, Edelman ER, Feldman CL, Stone PH. Role of endothelial shear stress in the natural history of coronary atherosclerosis and vascular remodeling: Molecular, cellular, and vascular behavior. J Am Coll Cardiol 2007;49:2379-93.
40. Zhang F, Lanning C, Mazzaro L, Barker AJ, Gates PE, Strain WD, *et al. In vitro* and preliminary *in vivo* validation of echo particle image velocimetry in carotid vascular imaging. Ultrasound Med Biol 2011;37:450-64.
41. Gurung A, Gates PE, Mazzaro L, Fulford J, Zhang F, Barker AJ, *et al.* Echo particle image velocimetry for estimation of carotid artery wall shear stress: Repeatability, reproducibility and comparison with phase-contrast magnetic resonance imaging. Ultrasound Med Biol 2017;43:1618-27.
42. Corti R, Fuster V. Imaging of atherosclerosis: Magnetic resonance imaging. Eur Heart J 2011;32:1709-19b.
43. Saho T, Onishi H. Evaluation of the impact of carotid artery bifurcation angle on hemodynamics by use of computational fluid dynamics: A simulation and volunteer study. Radiol Phys Technol 2016;9:277-85.
44. Sui B, Gao P, Lin Y, Gao B, Liu L, An J. Assessment of wall shear stress in the common carotid artery of healthy subjects using 3.0-tesla magnetic resonance. Acta Radiol 2008;49:442-9.
45. Garbey M, Pacull F. A versatile incompressible Navier-Stokes solver for blood flow application. Int J Numer Methods Fluid 2007;54:473-96.
46. Mynard JP, Wasserman BA, Steinman DA. Errors in the estimation of wall shear stress by maximum Doppler velocity. Atherosclerosis 2013;227:259-66.
47. Luntsi G, Ugwu AC, Nkubli FB, Emmanuel R, Ochie K, Nwobi CI. Achieving universal access to obstetric ultrasound in resource constrained settings: A narrative review. Radiography (Lond) 2021;27:709-15.
48. Tang D, Yang C, Walker H, Kobayashi S, Ku DN. Simulating cyclic artery compression using a 3D unsteady model with fluid-structure interactions. Comput Struct 2002;80:1651-65.
49. Tang D, Yang C, Kobayashi S, Zheng J, Vito RP. Effect of stenosis asymmetry on blood flow and artery compression: A three-dimensional fluid-structure interaction model. Ann Biomed Eng 2003;31:1182-93.
50. Onwuzu SWI, Ugwu AC, Onwuzu I, Agbo JA. Carotid Doppler indices with age and body mass index in a sampled Nigerian population. J Radiogr Radiat Sci 2021;35:43-9.
51. Ismail A, Ademola BL, Yusuf L, Abdulmalik MA. Renal arterial Doppler velocimetric indices among healthy subjects in North West Nigeria. J West Afr Coll Surg 2018;8:40-9.
52. Adamson SL, Morrow RJ, Langille BL, Bull SB, Ritchie JW. Site-dependent effects of increases in placental vascular resistance on the umbilical arterial velocity waveform in fetal sheep. Ultrasound Med Biol 1990;16:19-27.
53. Anderson DF, Bissonnette JM, Faber JJ, Thornburg KL. Central shunt flows and pressures in the mature fetal lamb. Am J Physiol 1981;241:H60-6.
54. Eze CU, Eze CU, Adeyomoye A. Sonographic evaluation of kidney echogenicity and morphology among HIV sero-positive adults at Lagos university teaching hospital. J Ultrasound 2018;21:25-34.
55. Atsukwei D, Eze ED, Chom ND, Igoh EO, Owoeye SC, Angbalaga A, *et al.* Correlation between abdominal ultrasonographic findings and CD4 cell count in adult patients with HIV/AIDS in Jos, Nigeria. Adv Mol Imag 2017;7:49-66.
56. Poelma C, Fraser KH. Enhancing the dynamic range of ultrasound imaging velocimetry using interleaved imaging. Meas Sci Technol 2013;24:1-3.
57. Poelma C. Ultrasound imaging velocimetry: A review. Exp Fluid 2017;58:1-28.
58. Fraser KH, Poelma C, Zhou B, Bazigou E, Tang MX, Weinberg PD. Ultrasound imaging velocimetry with interleaved images for improved pulsatile arterial flow measurements: A new correction method, experimental and in vivo validation. JR Soc Interface 2017;14:1-13.
59. von Reutern GM, Goertler MW, Bornstein NM, Del Sette M, Evans DH, Hetzel A, *et al.* Grading carotid stenosis using ultrasonic methods. Stroke 2012;43:916-21.